

Observation of orbitally excited (L=1) B mesons in $B^+ \rightarrow J/\psi K^+$ decays

Jennifer Pursley

April 15, 2004

Abstract

This proposal begins with a brief introduction to the Standard Model. Then the theory behind orbitally excited (L=1) B mesons is discussed, along with the importance of this observation for Heavy Quark Effective Theories and Same Side Tagging. Components of the Run II Collider Detector at Fermilab (CDF II) vital to the observation of B mesons are described. Preliminary results of an analysis search involving the observation of these B^{**} mesons in $J/\psi K^+$ decays are given. Finally, future research plans are outlined.

1 Standard Model

For decades, the Standard Model (SM) of Particle Physics has been the most complete theoretical description of particles and their interactions. Figure 1 tabulates the three generations of matter as well as the carriers of the three SM forces. Of these force carriers, the photon is the mediator of the electromagnetic force, the gluon of the strong force, and the Z and W bosons of the weak force. The fourth force, gravity, has yet to be included in the SM. Each elementary particle also has a corresponding antiparticle. Thus this table shows most of the fundamental particles in the SM.

All other forms of matter are composed of these fundamental particles. The strong force binds together quarks to form hadrons; the nature of the strong force is such that quarks can never be found in a free state. Most hadrons are formed of groups of one quark and one anti-quark (mesons) or three quarks (baryons). For example, the proton is a baryon composed of two up quarks and one down quark,

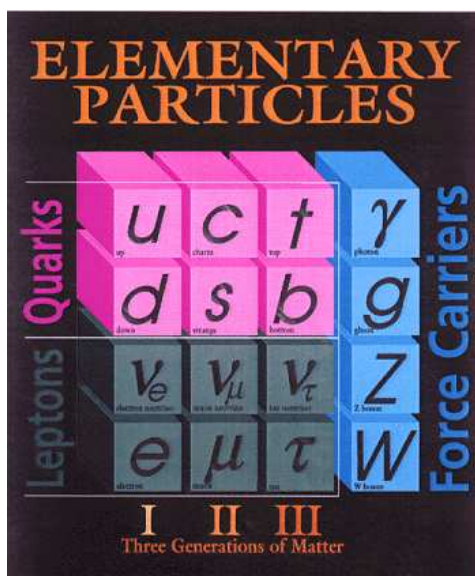


Figure 1: The three generations of matter [1].

denoted as uud . The B^{**} meson is formed of a down quark and an anti-bottom quark, denoted by $d\bar{b}$.

The SM as generally accepted remains incomplete. Not only does it fail to incorporate gravity, it also does not explain facts such as why there should be exactly three generations of matter or why the top quark is more than 35 times as massive as its partner, the bottom quark. Consequently, recent efforts in experimental particle physics focus primarily on measuring SM parameters to increasingly higher precision. Any deviation from predictions could indicate new physics beyond the SM.

2 B^{**} Theory

The B^{**} is not a single particle state; rather, it is composed of four orbitally excited ($L=1$) B^* mesons with nearly the same masses. Currently the Particle Data Group (PDG), an international organization which collates all particle physics results, lists no experimental results for the masses or widths of the B^{**} . Theoretical predictions on the masses vary, and no conclusive predictions for the widths are known in any theory.

Name	\mathbf{J}	J_q	Mass (GeV/c^2)			Width MeV	Decay Mode
			EHQ [2]	ref. [3]	EGF [4]		
B_0^*	0	$\frac{1}{2}$	5.650	5.870	5.738	100	$(B\pi)_{L=0}$
B_1^*	1	$\frac{1}{2}$	5.650	5.875	5.757	100	$(B^*\pi)_{L=0}$
B_1^*	1	$\frac{3}{2}$	5.759	5.700	5.719	20	$(B^*\pi)_{L=2}$
B_2^*	2	$\frac{3}{2}$	5.771	5.715	5.733	24	$(B\pi, B^*\pi)_{L=2}$

Table 1: Table replicated from [5].

The three mass columns in Table 1 are the B^{**} masses calculated using three different Heavy Quark Effective Theories: Effective Heavy Quark (EHQ) [2], a non-relativistic valence quark theory [3], and a fully relativistic valence quark theory (EGF) [4]. The widths of the two narrow peaks were calculated by EHQ; there is no clear evidence for the actual widths of the two wide peaks. As depicted by Fig. 3, in all three of these theoretical predictions the two narrow peaks are so near to each other that they merge into one peak. Naturally the two wide peaks also merge into one wide peak underlying the narrower peak. From these predictions, we can determine the shape of the mass peaks we expect to see and ‘float’ the locations of these shapes when fitting real data.

2.1 Heavy Quark Effective Theories (HQET)

The basis for all HQET is Heavy Quark Symmetry. In mesons composed of one heavy quark and one light quark, the heavy quark’s mass can be approximated as infinite. This symmetry greatly simplifies first-order calculations of the meson’s mass and width. HQET explained the unexpectedly narrow D^{**} ($c \bar{u}$) states, and has been extrapolated to predict the B^{**} states [6]. The valence quark theories combine Heavy Quark Symmetry with different dynamical models of the light quark in the meson. Observation of the B^{**} states will test the predictions of these various theories.

2.2 Same Side Tagging (SST)

SST is the search for pions produced along with B mesons. The pions will be charge-correlated with the accompanying B meson, making it possible to tag the flavor of the B meson at production. Flavor tagging is used to detect oscillations (mixing) between B^0 ($d \bar{b}$) and \bar{B}^0 ($\bar{d} b$) states. These correlated pions come from

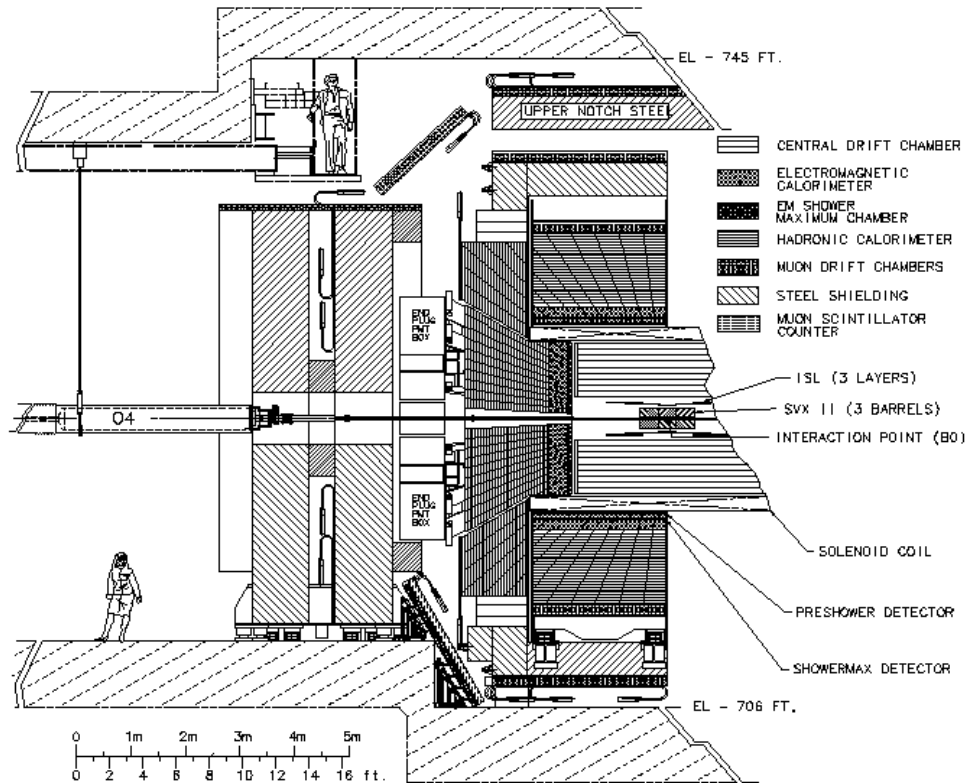


Figure 2: Elevation view of one half of the CDF II. Beam runs along the z-axis, from left to right.

two different sources: the decay of B^{**} excited states, and fragmentation of the b-quark. Other experiments have shown that approximately 30% of the B mesons produced at CDF II come from B^{**} decay. Thus the B^{**} datasets will be useful in SST studies.

3 Collider Detector at Fermilab (CDF II)

CDF II (Fig. 2) is a general purpose solenoidal detector. It combines precision charged particle tracking with fast projective calorimetry and fine grained muon detection. CDF II began operation in March 2001, with the Tevatron colliding protons and antiprotons ($p \bar{p}$) at a center-of-mass energy just under 2.0 TeV. By

Sept. 2003, CDF II had collected 220 pb^{-1} of data, including some of the world's largest samples of various B meson decays. The components of the detector most relevant to the B^{**} search in $J/\psi K^+$ decays are the Silicon Vertex Detector (SVX II), the Central Outer Tracker (COT), and the muon systems.

The SVX II and the COT are both located within a superconducting solenoid which produces a magnetic field of 1.4 Tesla parallel to the beam axis. The SVX II is a solid-state silicon detector consisting of 5 cylindrical silicon layers extending out to a radius of 11 cm. Outside the SVX II are the Intermediate Silicon Layers (ISL) which extend silicon coverage farther in the forward direction and out to a radius of 28 cm. These silicon detectors provide tracking information close to the beamline and allow precise resolution of decay vertices.

The COT is an open cell wire drift chamber which covers radii between 44 and 132 cm. The COT is comprised of 8 cylindrical superlayers. The superlayers are made up of separate drift cells, each containing 12 high-voltage sense wires. Four superlayers contain wires oriented axially; the remaining four have small angle stereo wires. This provides up to 96 measurements between 44 and 132 cm and allows tracking in both the polar (η) and azimuthal (ϕ) directions.

The scintillator based calorimeters measure electron and photon energies, jet energies, and net transverse energy flow. The electromagnetic (EM) section is composed of alternating layers of lead and scintillator, designed to stop electrons and photons. The hadron section is made from layers of iron and scintillator to stop the heavier hadrons. Muons, which are massive and weakly interacting, pass through these two layers and into the muon chambers. The muon system uses scintillators and proportional drift chambers to detect and track muons.

4 Preliminary Analysis Results

In this search, we reconstructed B^{**} in the channel

$$B^{**} \rightarrow B^+ \pi^- (B^+ \rightarrow J/\psi K^+, J/\psi \rightarrow \mu^+ \mu^-)$$

The analysis used the first 220 pb^{-1} of CDF II data with two outgoing muons. Additional cuts made on the data are listed in Table 2. Of the cut variables listed, p_T is the transverse momentum, L_{xy} is the transverse decay length and d_0 is an impact parameter, defined as the distance of closest approach to the beam-spot. The mass of the J/ψ was also constrained to its exact PDG value in our baseline analysis dataset. The benefit of this is more accurate vertex measurements with small loss of events.

Particle	Cut	Cut Value	Units
Track Quality	Silicon Hits ($r - \phi$)	> 3	GeV/c
	COT axial hits	> 20	
	COT stereo hits	> 16	
	p_T	> 0.5	
μ^\pm	Two opposite charge μ	$p_T > 1.5$	GeV/c
J/ψ	$ m(J/\psi) - 3.095 $	< 0.04	GeV/c ²
K	p_T	> 2.0	GeV/c
B	$ m(B) - 5.28 $	< 0.04	GeV/c ²
	p_T	> 6.5	GeV/c
	L_{xy}	> 100	microns
	$L_{xy}/\sigma_{L_{xy}}$	> 7	
π	p_T	> 0.9	GeV/c
	$ d_0/\sigma_{d_0} $	< 3	
B^{**}	$m(B^{**})$	> 5.2	GeV/c ²
	$m(B^{**})$	< 7.2	GeV/c ²
	p_T	> 5.0	GeV/c

Table 2: Summary of baseline analysis cuts. B reconstruction cuts based on [7].

The result of the B^{**} mass from this search is plotted in Fig. 4. In this figure, the black line is for events which produced the right sign; the charge of the B^{**} , $Q(B^{**})$, was 0. The red line indicates events which found a B^{**} with the wrong sign, $Q(B^{**}) = \pm 2$. This occurs when the kaons and pions found are a result of fragmentation surrounding the production of the b-quark, not a true B^{**} production event. Thus the wrong sign plot contains only fragmentation events and should have approximately the same shape as the background in the right sign plot [5]. This plot also uses the same x-axis as the theoretical prediction plots in Fig. 3. Comparing Figs. 3 and 4, we see a definite excess of events in the right sign plot in the same region as we would expect to see a B^{**} mass peak.

5 Future Research

While these results appear promising, they are still far from conclusive. The next step in the analysis to generate a realistic Monte Carlo (MC) simulation of this decay. With this MC sample we will fit shapes for the B^{**} mass peaks, which we

can then float in the fit on real data. Additionally, properly tuned realistic MC will predict the expected background signal around the mass peaks, allowing us to judge our ability to see the wide peaks above the background.

Comparing pure MC signal to a background data sample also makes it possible to choose cuts which optimize the signal/background ratio in real data. The current baseline analysis cuts are based on previously optimized cuts [7], but have not been optimized specific to this analysis. Once these MC studies have been performed, we will run over data again with the optimized cuts.

We can also boost the statistics on the B^{**} by pursuing other B decay modes. There are many hadronic decay modes with higher statistics than the $J/\psi K$ modes; one mode which we have already begun to investigate is

$$B^{**} \rightarrow B^+ \pi^- (B^+ \rightarrow D^0 \pi^+, D^0 \rightarrow K^+ \pi^-)$$

Higher statistics will improve the quality of the fit and make the results more conclusive overall.

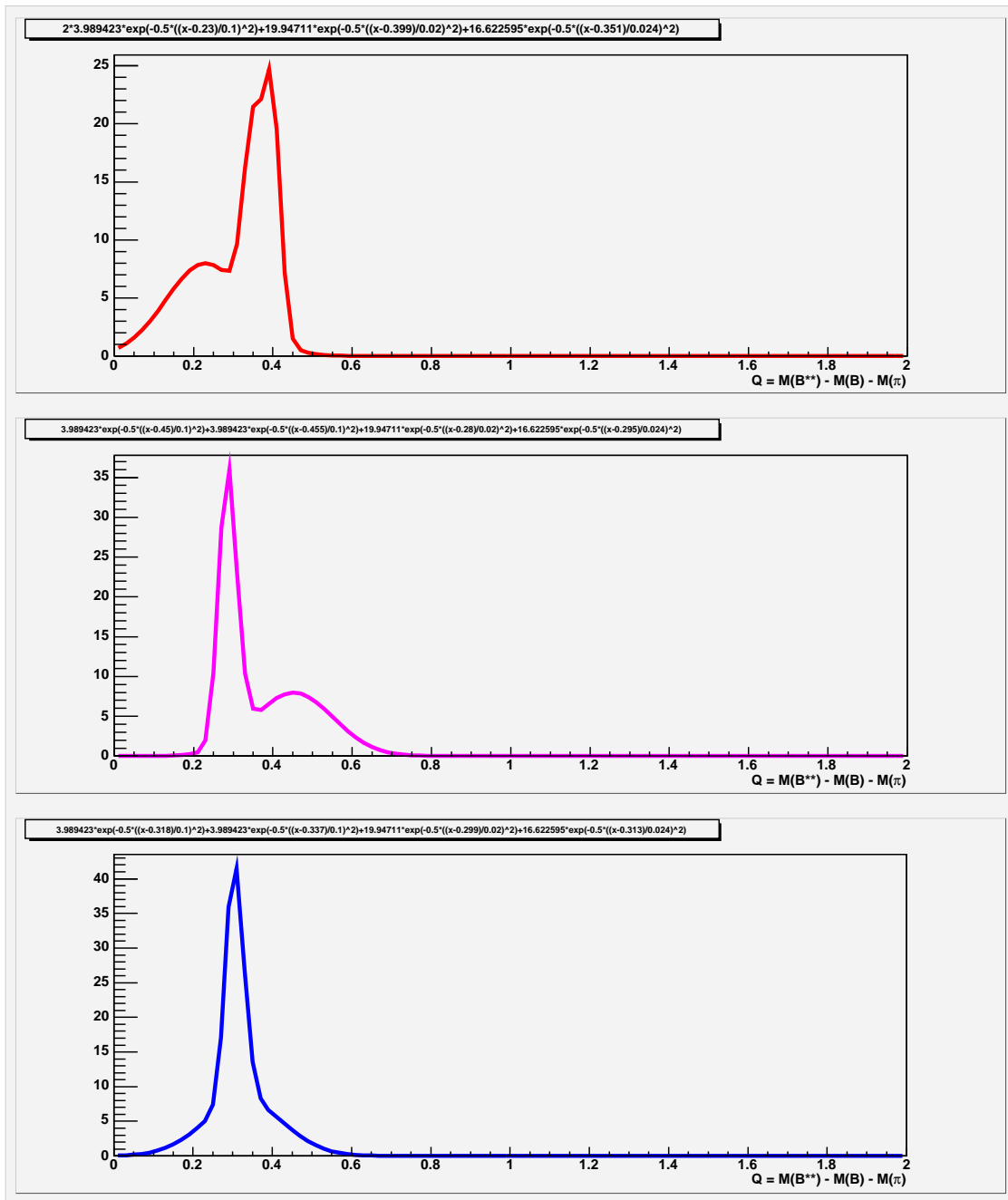


Figure 3: Plot of the three theoretical predictions of B^{**} resonances. Top: EHQ; middle: nonrelativistic; bottom: EGF.

Right vs. Wrong Sign

right_sign	
Entries	876
Mean	0.8381
RMS	0.5052

$B^{**} \rightarrow B \pi, B \rightarrow J/\Psi K, J/\Psi \rightarrow \mu\mu$
 J/Ψ mass constrained to PDG value
 $\text{abs}(\text{Psi.Fmass}-3.095)<0.04 \ \&\& \ \text{abs}(\text{Bu.F2mass}-5.28)<0.04 \ \&\& \ \text{K.F2pt}>2 \ \&\& \ \text{Bu.F2pt}>6.5$
 $\&\& \ \text{Bu.Lxy}>0.01 \ \&\& \ \text{Bu.LxyS}>7 \ \&\& \ \text{abs}(\text{Pi.d0s})<3 \ \&\& \ \text{Pi.pt}>0.6$

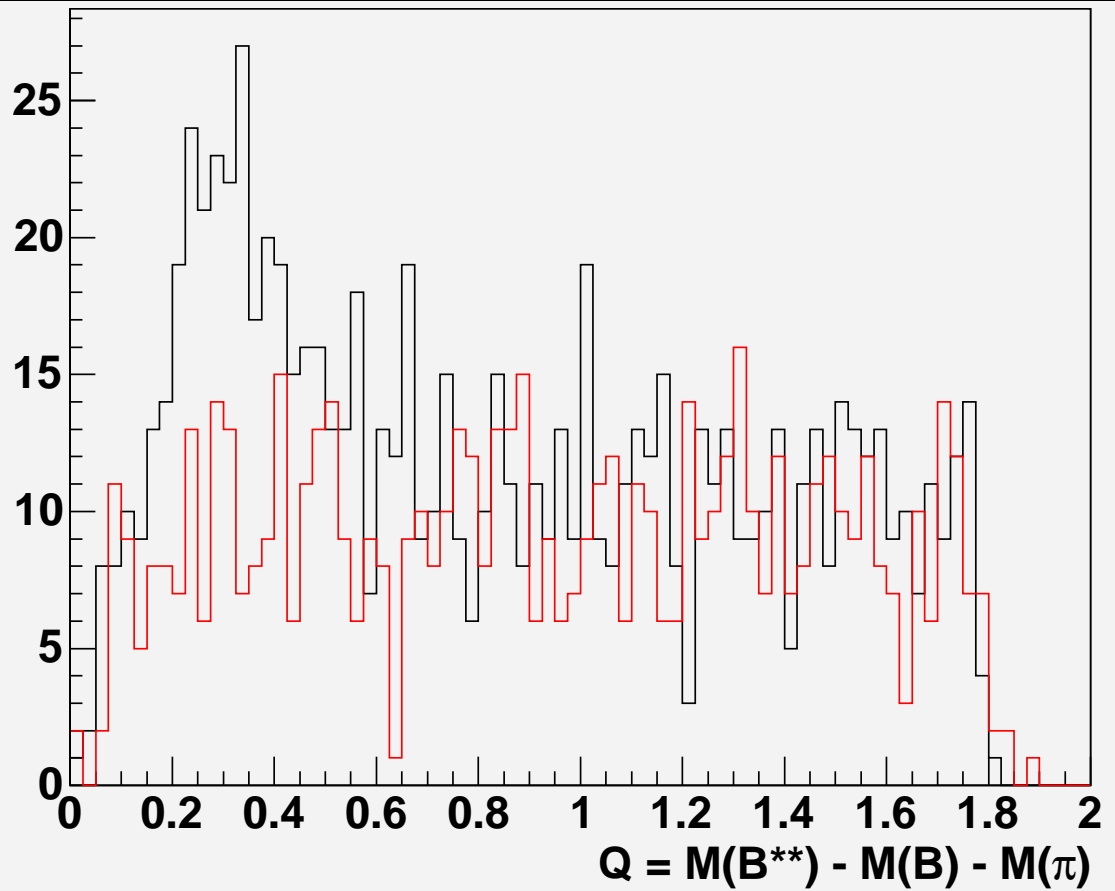


Figure 4: Plot of $m(B^{**}) - m(B) - m(\pi)$ for 220 pb^{-1} of data.

References

- [1] J. Schombert, Oct. 2003. Retrieved April 06, 2004 from <http://zebu.uoregon.edu/js/ast123/lectures/lec08.html>.
- [2] E. Eichten, C. Hill, C. Quigg, “Properties of Orbitally Excited Heavy-Light Mesons,” *Phys. Rev. Lett.* 71, 25 (1993); “Orbitally Excited Heavy-Light Mesons Revisited,” FERMILAB-CONF-94/118-T (1994).
- [3] N. Isgur, “Spin-Orbit Inversion of Excited Heavy Quark Mesons,” JLAB-THY-97-26.
- [4] D. Ebert, V. O. Galkin, R. N. Faustov, “Mass spectrum of orbitally and radially excited heavy-light mesons in the relativistic quark model,” hep-ph/9712318, HUB-EP-97/90 (1997), and references therein.
- [5] D. Vucinic, “Observation of Excited B Mesons in p-pbar Collisions at $\sqrt{s} = 1.8$ TeV”, PhD thesis, 1998, Massachusetts Institute of Technology. Retrieved Jan. 15, 2004 from <http://www-cdf.fnal.gov/htbin/cdfnoteSelNum?number=4817>.
- [6] A. Falk, T. Mehen, “Excited Heavy Mesons Beyond Leading Order in the Heavy Quark Expansion,” JHU-TIPAC-950008, hep-ph/9507311 (1995).
- [7] A. Korn, Ch. Paus, D. Starr, “Update on the Measurement of B Meson Masses in the Exclusive J/ψ Channels,” CDF Note 6426 (April 2003), and references therein.